THE JOURNAL OF PHYSICAL CHEMISTRY C

Article

pubs.acs.org/JPCC

Sharp Fickian Behavior of Electrogenerated Chemiluminescence Waves in Conjugated Polymer Films

David A. Edwards*

Department of Mathematical Sciences, University of Delaware, Newark, Delaware 19716-2553, United States

ABSTRACT: One technique to study electrochemical oxidation phenomena in thin polymer films is the generation of electrogenerated chemiluminescence (ECL) waves. Such waves are sharp and easy to image, and recent experiments have shown both constant-speed and Fickian-style wave behavior. One way to model such waves mathematically is to track the concentration of the ion clusters in the polymer film. One such model has a standard Fickian form but with a highly nonlinear diffusion coefficient. This model is analyzed numerically, and the results are compared with previous asymptotic analysis. The results demonstrate that ECL waves corresponding to this model are indeed sharp and move in a Fickian way. Hence more complicated effects must be included in the model if constant-speed behavior is to be observed.

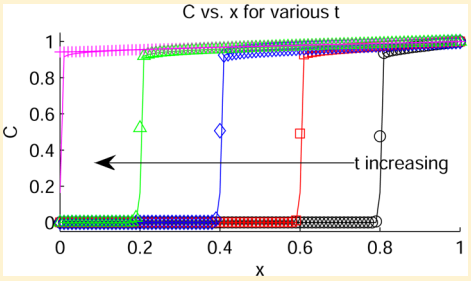

1. INTRODUCTION

Electrochemical conjugated polymer films show great promise for advances in many technologies. These films can be used in electrochromic "smart" windows that control the level of transparency as voltage is applied.[1] Such films are used in many types of sensors, including those used for detecting chemicals, determining humidity and pH, and mimicking human senses.[2] They form the basis for organic light-emitting diodes (OLEDs),[3] which are used to create screens for small electronics and now even televisions.[4] Because oxidation and reduction can change the volume of polymer films, one can exploit this process to create electrochemical actuators[5] or even artificial muscles.[6] A robust knowledge of the behavior of the underlying kinetics is crucial to controlling and optimizing such devices.

One useful approach to studying these devices is through electrogenerated chemiluminescence (ECL),[7] which allows optical study of the reduction and oxidation processes. A key feature of these processes is the formation of a sharp front in the concentration of ionic clusters, which causes bright patterns in ECL experiments.[8] This behavior has already been exploited industrially for use in fingerprinting devices.[9]

Given a source of clusters, this front propagates with time; hence these patterns are sometimes referred to as "ECL waves" or "ECL solitons".[10,11] One key quantity to determine is the speed at which these waves propagate. For many years, experiments have shown sharp fronts in such systems;[12] however, some experiments show the front moving proportional to $\sqrt{t}$, as one would expect from a purely diffusive process,[13] whereas others claim to see the front moving with constant speed,[14,15] as one might expect from including the effects of swelling and other changes in the polymer matrix.[16−18] Still others see the front moving in both ways depending on experimental parameters.[19]

Most current models for ECL systems include only diffusive effects,[20] although several have highly nonlinear diffusion coefficients.[21] Because Fickian models allow similarity solutions depending on $x/\sqrt{t}$, it is unlikely that such models can capture constant-speed behavior.[21]

In Guo et al.,[8] the authors study the oxidation of a thin poly(9,9-dioctylfluorene-*co*-benzothiadiazole) film. The film is embedded with an array of Au electrode posts that provide nucleation sites for ionic clusters that spread through the film, causing the ECL waves. The authors claim that their numerical simulations show sharp fronts moving with constant speed; however, asymptotic analysis of the same model shows that the sharp fronts move like $\sqrt{t}$.[22] We shall use a numerical scheme to verify those asymptotic results and explain the discrepancy between the two groups.

2. RESULTS AND DISCUSSION

2.1. Governing Equations. The full description of the experiment under consideration is provided in Guo et al.;[8] below we summarize the details relevant for analyzing the resulting system. The ECL wave is modeled through the concentration C of ionic clusters in a thin ($\approx$ 250 nm) film made of poly(9,9-dioctylfluorene-*co*-benzothiadiazole). The governing (dimensionless) equation is the following:

$$\frac{\partial C}{\partial t} = \frac{\partial}{\partial x}\left[D(C)\frac{\partial C}{\partial x}\right] \tag{1a}$$

$$D(C) = \frac{D_w}{1 + e^{-\kappa(C-C_T)}} + D_d \tag{1b}$$

where the subscripts "w" and "d" refer to "wet" and "dry". Here x measures distance along the film and C_T is a saturation

Received: January 15, 2013
Revised: March 7, 2013
Published: March 7, 2013

concentration, so we consider the region where $C > C_T$ to be "wet". Initially, there are no clusters in the polymer, so

$$C(x, 0) = 0 \tag{2}$$

In the experiments by Guo et al.,[8] Au posts at $x = \pm 1$ provide (the same) constant concentration of clusters, which is higher than the saturation concentration. These boundary conditions are even in x, as are eqs 1a, 1b, and 2. Hence we may exploit this symmetry to take the interval as $x \in [0,1]$ with

$$\frac{\partial C}{\partial x}(0, t) = 0 \tag{3a}$$

$$C(1, t) = 1, \quad C_T < 1 \tag{3b}$$

Note that the interval $[0,1]$ is generic. If the posts were spaced $2L$ units apart, then we could define a new variable $y = x/L$ and obtain our previous system with a scaled value of $D(C)$.

With a diffusion coefficient of the form in eq 1b, making κ large causes a great change in the size of the diffusion coefficient as the polymer changes from dry to wet. Hence we would like to examine the solution of eqs 1a and 1b for large κ. Moreover, D_d is usually quite small; in particular, Guo et al. indicate that D_d can be up to six orders of magnitude smaller than D_w.[8] To reduce the number of perturbation parameters under consideration, we take

$$\frac{D_d}{D_w} = \frac{D_*}{\kappa} \tag{4}$$

where D_* is considered to be $O(1)$. Substituting eq 4 into eq 1b, we obtain

$$D(C) = D_w\left[\frac{1}{1 + e^{-\kappa(C-C_T)}} + \frac{D_*}{\kappa}\right] \tag{5}$$

which varies only with κ.

A graph of $D(C)$ on a logarithmic scale is shown in Figure 1. The parameters chosen are similar to those in Guo et al.[8] to replicate the sharp ECL waves seen experimentally.[13−15,19] In particular, we choose

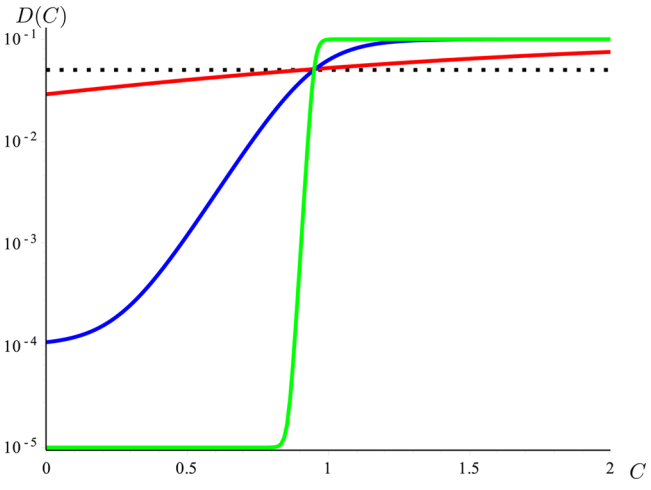

Figure 1. $D(C)$ versus C on a logarithmic scale. Here $C_T = 0.95$, $D_w = 0.1$, and $D_* = 0.01$. Dotted line: $D(C)$ given by eq 1b with $\kappa = 0$. Solid curves: $D(C)$ given by eq 5 with $\kappa = 1$, 10, and 100 . Note that as κ increases, the curve steepens and the diffusion coefficient in the dry region decreases.

$$C_T = 0.95, \quad D_w = 0.1, \quad D_* = 0.01 \tag{6}$$

Note that with $\kappa = 0$, we have D constant. Note also that as κ increases the curve gets steeper and D_d gets smaller. In fact, for very large κ, one can think of $D(C)$ as being piecewise constant (at least to leading order).

2.2. Asymptotic Solution. In Edwards,[22] the author constructs the solution of this system for large κ; we summarize the results here. First, introduce the similarity variable

$$\zeta = \frac{1 - x}{2\sqrt{D_w t}} \tag{7}$$

Note that if the solution can be shown to depend only on ζ (which we do below), then the isoclines of C (which correspond to ECL waves) will move like $\sqrt{t}$, as consistent with standard Fickian behavior. In particular, we define $\zeta = \zeta_s$ to be the isocline corresponding to the saturation value at leading order:

$$C(\zeta_s) = C_T \tag{8}$$

In this formulation, there are five separate regions of interest, as shown in Figure 2. Note that three of these regions are very

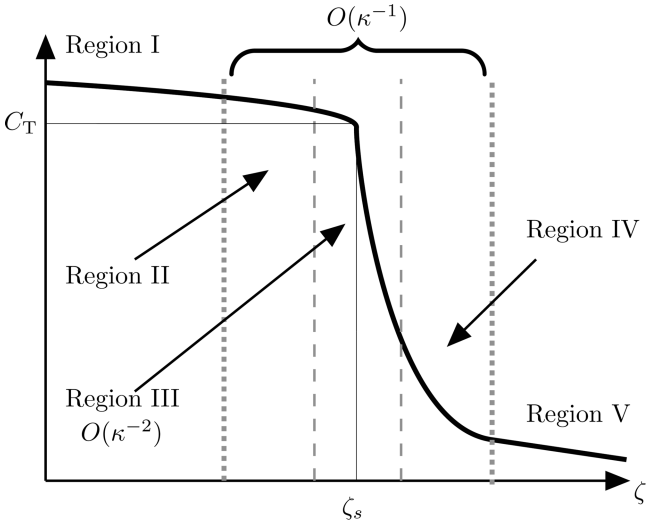

Figure 2. Schematic of various regions with different behavior in the diffusion coefficient.

thin, depend on the size of κ, and exist around $C = C_T$, which is where the diffusion coefficient changes rapidly in Figure 1. Hence each region corresponds to different behaviors in eq 5:

- In Region I, the concentration is far enough above C_T that the exponential term in the numerator of the first bracketed term goes to zero. Hence the bracketed term is ~1, $D(C) \approx D_w$, and the evolution proceeds as if the diffusion coefficient was constant.
- In Region II, the concentration is near enough to C_T that the nonlinear term in eq 5 must be considered but not the D_* term.
- In Region III, both terms in eq 5 are of the same size.
- In Region IV, C is far enough below C_T that $D(C) \approx D_d$, and the evolution proceeds as if the diffusion coefficient is constant. In particular, there is a sharp transition in the concentration between the saturation value and zero.
- In Region V, C is exponentially small, which means that the polymer can be considered to be essentially dry.

dx.doi.org/10.1021/jp400476m | J. Phys. Chem. C 2013, 117, 6747−6751

Because of the structure discussed above, the similarity-variable solution is a good approximation only when region V (with its exponentially small flux) contains the boundary $x = 0$, where eq 3a is applied. Hence the similarity transformation will work only until $t_{max} = (4\zeta_s^2 D_w)^{-1}$; after that the wet solution occupies the entire domain.

Because of the different regions, we must break the solution into two parts. In the dry region where $\zeta > \zeta_s$, the solution is given by[22]

$$C(\zeta) = C_T\left[\exp\left(-\frac{2\zeta_s\kappa(\zeta-\zeta_s)}{D_*}\right) + \frac{2\zeta_s\kappa(\zeta-\zeta_s)}{D_*}\right] - \frac{\log\kappa}{\kappa} - \frac{u_c(\zeta)}{\kappa}, \quad \zeta > \zeta_s \tag{9a}$$

where we must restrict the domain on ζ because the exponential term in eq 9a will diverge for $\zeta > \zeta_s$. u_c may be defined implicitly through

$$D_* u_c - e^{-u_c} = 2\zeta_s C_T \kappa^2(\zeta - \zeta_s) + A \tag{9b}$$

or written explicitly in terms of the Lambert W function.[23] Here A is a constant yet to be determined.

In the wet region, the solution is given by

$$C(\zeta) = 1 - (1 - C_T)\frac{\operatorname{erf}\zeta}{\operatorname{erf}\zeta_s} + \frac{1}{\kappa}\log\left(\frac{1 - e^{-2\kappa\zeta_s C_T(\zeta_s-\zeta)}}{2\kappa\zeta_s C_T(\zeta_s - \zeta)}\right) - \frac{\log\kappa}{\kappa} - \frac{u_c(\zeta)}{\kappa}, \quad \zeta < \zeta_s \tag{10}$$

The two solutions 9a and 10 match at $\zeta = \zeta_s$, with a smooth derivative, as required. ζ_s itself is given by the following equation, which arises from balancing the flux at $\zeta = \zeta_s$

$$(1 - C_T)e^{-\zeta_s^2} = (C_T\zeta_s \operatorname{erf}\zeta_s)\sqrt{\pi} \tag{11}$$

Note that eq 11 is independent of D_w (because that dependence is scaled away in the definition of ζ).

2.3. Numerical Simulations. We implement a numerical solution to check the asymptotic approach. First, we note that if we define

$$F(x, t) = D_d C(x, t) + \frac{D_w}{\kappa}\log(1 + e^{\kappa[C(x,t)-C_T]}) \tag{12}$$

then

$$\frac{\partial F}{\partial x} = \left\{D_d + \frac{D_w}{\kappa}\frac{\kappa e^{\kappa[C(x,t)-C_T]}}{1 + e^{\kappa[C(x,t)-C_T]}}\right\}\frac{\partial C}{\partial x} = D(C)\frac{\partial C}{\partial x} \tag{13}$$

and eq 1a becomes

$$\frac{\partial C}{\partial t} = \frac{\partial^2 F}{\partial x^2} \tag{14}$$

which provides a natural way to discretize the problem using a conservative scheme. Because we will be applying spatial differences to F, we need boundary conditions for it:

$$\frac{\partial F}{\partial x}(0, t) = 0 \tag{15a}$$

$$F(1, t) = D_d + \frac{D_w}{\kappa}\log(1 + e^{\kappa(1-C_T)}) \tag{15b}$$

where we have used eqs 3a and 3b.

We discretize by letting

$$F_{i,j} = F\left(\frac{(i-1)}{N}, (j-1)\Delta t\right), \quad i = 1, ..., N+1, \quad j \geq 1 \tag{16}$$

and similarly for C. From the x discretization in eq 16 we have found that $\Delta x = N^{-1}$. Because of the nonlinearity in F, any implicit method would require a nonlinear solver like Newton's method. Instead, we choose the explicit method

$$\frac{C_{i,j+1} - C_{i,j}}{\Delta t} = \frac{F_{i-1,j} - 2F_{i,j} + F_{i+1,j}}{(\Delta x)^2} \tag{17}$$

For a diffusion equation with constant D, the following constraint must be satisfied to guarantee convergence (cf. Sauer,[24] Theorem 8.2):

$$\Delta t < \frac{(\Delta x)^2}{2D} \tag{18}$$

For our problem, the most conservative estimate for eq 18 uses the largest value taken on by $D(C)$ (namely, $D_w + D_d$), so to ensure convergence we take $\Delta t = (3D_w N^2)^{-1}$.

By using the standard approach of introducing a "phantom point" at $-\Delta x$ to take care of the Neumann condition 15a, we see that the algorithm 17 may be written in matrix-vector notation as

$$\mathbf{C}_{j+1} = \mathbf{C}_j + M\mathbf{F}_j; \quad \mathbf{C}_j, \mathbf{F}_j \in \mathcal{R}^{n+1}; \quad M \in \mathcal{R}^{(n+1)\times(n+1)} \tag{19a}$$

$$M = \frac{1}{3D_w}\begin{pmatrix} -2 & 2 & 0 & 0 & \cdots & 0 & 0 & 0 \\ 1 & -2 & 1 & 0 & \cdots & 0 & 0 & 0 \\ \vdots & \vdots & \vdots & \vdots & \ddots & \vdots & \vdots & \vdots \\ 0 & 0 & 0 & 0 & \cdots & 1 & -2 & 1 \\ 0 & 0 & 0 & 0 & \cdots & 0 & 0 & 0 \end{pmatrix} \tag{19b}$$

Here the last row of M is all zeroes because $C_{n+1,j} = 1$ for all t from the boundary condition 3b.

To validate the algorithm, we began by simulating the case where $\kappa = 0$. In this case, the diffusion coefficient is constant and an exact solution can be found using separation of variables. Numerical simulations showed agreement with error proportional to N^{-2}, as predicted by the theory.[24]

Next, we check the accuracy of the asymptotic solution for the full problem against the numerical simulations with $N = 100$. In particular, with the parameters given in eq 6, we have found that

$$\zeta_s = 0.1608, \quad t_{max} = 96.6552 \tag{20a}$$

For κ, motivated by Guo et al.,[8] we select a value large enough to reproduce the sharp ECL waves seen experimentally:[13−15,19]

$$\kappa = 100 \Rightarrow D_d = 10^{-5} \tag{20b}$$

where we have used eqs 4 and 6.

The final parameter to be identified is A. From standard asymptotic matching practice, A would be determined by the next term in the dry solution [which is $O(\kappa^{-1})$]. When comparing with numerics, an equivalent approach is to require that the numerical and asymptotic solutions match at the dry boundary. Hence we matched the asymptotic value of $C(0,\Delta t)$ to the numerical value, yielding $A = -0.01461$.

dx.doi.org/10.1021/jp400476m | J. Phys. Chem. C 2013, 117, 6747−6751

Clearly a key question is whether the ECL wave moves with constant speed, as claimed in Guo et al.,[8] or like $\sqrt{t}$, consistent with the Fickian theory. In Figure 3, we plot the evolution of

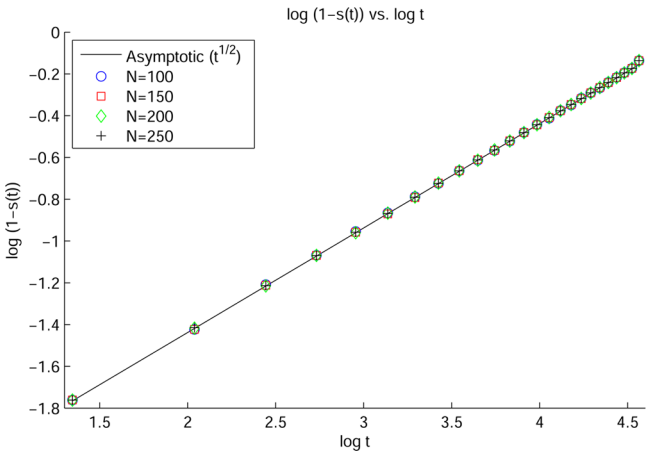

Figure 3. Comparison of asymptotic and numerical solutions (for various values of N) for the isocline $s(t)$, where $C(s(t),t) = C_T$, demonstrating that it moves proportional to $\sqrt{t}$, consistent with Fickian behavior. $1 - s(t)$ is plotted because the front moves from right to left.

the isocline where $C = C_T$. Because we are now considering the full asymptotic solution as given by eqs 9a, 9b, and 10, we track the isocline directly, rather than using the leading-order approximation 8. The Figure presents the results from numeric and asymptotic cases; for each, linear interpolation between grid points was used to estimate the position of $s(t)$, where $C(s(t),t) = C_T$.

By definition, the isocline for the asymptotic solution behaves like $\sqrt{t}$, as shown by the solid curve in Figure 3. Note the very close agreement with the numerical solution, showing that the front does indeed behave like $\sqrt{t}$, at least until the entire polymer saturates (rightmost data in Figure 3). Note that the numerically computed front values are the same for each N, as one would expect from a convergent numerical scheme.

Although this $\sqrt{t}$ dependence contradicts the conclusion of Guo et al.,[8] it is actually compatible with their results. In Figure S2 of appendix I in the supporting information to their work, the authors show that the front speed decreases inversely with the step size Δx. Suppose that the front $s(t)$ advances $\Delta s = m\Delta x$ over a time step Δt. Then, their data imply that

$$\frac{\Delta s}{\Delta t} = \frac{m\Delta x}{\Delta t} \propto \frac{1}{\Delta x} \Rightarrow \frac{\Delta s}{\Delta t} \propto \frac{1}{\sqrt{\Delta t}}$$

as expected from Fickian dynamics.

Next, we compare the actual solution profiles from the asymptotic and numerical solutions to see if they show the type of sharp front profile seen experimentally.[13−15,19] In Figure 4, we plot a series of snapshots in time comparing the numerical and asymptotic solutions. The time intervals are chosen so that the front moves a fixed distance between snapshots. Note the close agreement between the numerical and asymptotic solutions, with significant differences visible only for the last time snapshot. Although it is difficult to discern due to the narrow width of the front, the solutions also exhibit a "shoulder-like" profile, as a very sharp bend in the wet polymer

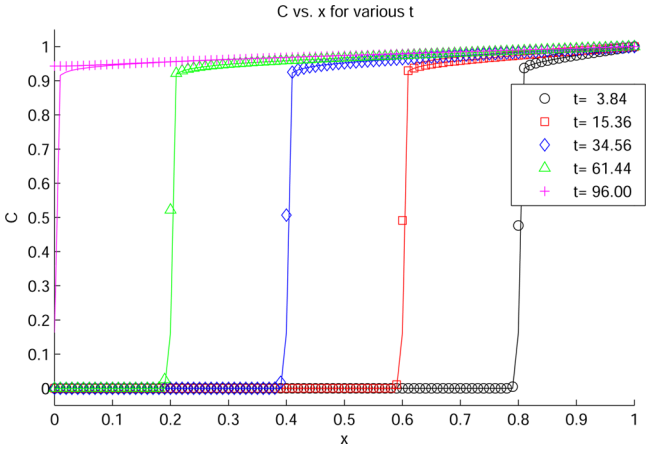

Figure 4. Concentration profiles from the numeric (symbol) and asymptotic (line) solutions for various times. Note the sharp nature of the front. The time intervals are chosen so that the front moves a fixed distance between snapshots.

transitions to a much wider profile in the dry region,[22] which is reminiscent of experimental data for these systems.[13−15,19]

3. CONCLUSIONS

One way for scientists to better understand the oxidation processes in polymer films is through ECL. Although experimental data consistently show sharp ECL waves in such systems, there is debate as to whether those waves—which correspond to concentration isoclines of ionic clusters—move like t or $\sqrt{t}$.[14,15,19] Certainly diffusion in polymers can exhibit sharp fronts moving with constant speed, as found by Thomas and Windle,[18] although typically the mathematical models for such behavior must include other effects beside nonlinear Fickian diffusion.[16,17]

In Guo et al.,[8] the authors propose a nonlinear Fickian-type model for ECL waves and claim that their simulations show the model allows for constant front speed. In this work, we examined the model numerically, compared these results with the asymptotic solutions in Edwards,[22] and demonstrated that although the nonlinear diffusion coefficient does produce sharp fronts, those fronts still move proportional to $\sqrt{t}$.

In the limit of large κ, the domain can be divided into several separate regions, where different processes dominate. Far from the ionic source, a nearly dry precursor region permits the use of a similarity-variable solution, which forces the front to behave like $\sqrt{t}$. The nearly piecewise-constant behavior of $D(C)$ for large κ forces a sharp front near the saturation value. In the bulk of the wet region, the diffusion coefficient is a constant D_w, and the dynamics are again standard Fickian.

In this work, we implemented a conservatively differenced explicit numerical method to solve eqs 1a and 1b subject to eqs 2, 3a, and 3b to compare with the theoretical work in Edwards.[22] The results from the asymptotic and numeric approaches agree, showing a sharp front moving proportional to $\sqrt{t}$, profiles that agree well with experimental results.[13−15,19]

Although the analysis in this article focused on the model from Guo et al.,[8] the conclusions are quite general. Consider any model of the form 1a subject to eqs 2 and 3a and 3b. As long as the diffusion coefficient in the dry region is negligible, an $x/\sqrt{t}$ similarity variable can be used, no matter the exact functional form of $D(C)$. Hence to capture constant front speed in ELC waves, one has to incorporate additional effects that

dx.doi.org/10.1021/jp400476m | J. Phys. Chem. C 2013, 117, 6747−6751

arise due to the nature of the polymer film, such as viscoelastic stresses in the polymer.[16,17]

AUTHOR INFORMATION

Corresponding Author

*E-mail: edwards@math.udel.edu.

Notes

The authors declare no competing financial interest.

ACKNOWLEDGMENTS

The author thanks the reviewers for their many insightful suggestions.

REFERENCES

(1) Rauh, R. Electrochromic Windows: An Overview. *Electrochim. Acta* **1999**, *44*, 3165−3176. 3rd International Meeting on Electrochromics (IME-3), Imp. Coll., London, Sept 7−9, 1998.

(2) Adhikari, B.; Majumdar, S. Polymers in Sensor Applications. *Prog. Polym. Sci.* **2004**, *29*, 699−766.

(3) Armstrong, N.; Wightman, R.; Gross, E. Light-Emitting Electrochemical Processes. *Annu. Rev. Phys. Chem.* **2001**, *52*, 391−422.

(4) van der Vaart, N.; Lifka, H.; Budzelaar, F.; Rubingh, J.; Hoppenbrouwers, J.; Dijksman, J.; Verbeek, R.; van Woudenberg, R.; Vossen, F.; Hiddink, M.; Rosink, J.; Bernards, T.; Giraldo, A.; Young, N.; Fish, D.; Childs, M.; Steer, W.; Lee, D.; George, D. Towards Large-Area Full-Color Active-Matrix Printed Polymer OLED Television. *J. Soc. Inf. Disp.* **2005**, *13*, 9−16. International Symposium of the Society for Information Display (SID 2004), Seattle, WA, May 25−27, 2004.

(5) Jager, E.; Smela, E.; Inganas, O. Microfabricating Conjugated Polymer Actuators. *Science* **2000**, *290*, 1540−1545.

(6) Smela, E. Conjugated Polymer Actuators for Biomedical Applications. *Adv. Mater.* **2003**, *15*, 481−494.

(7) Richter, M. Electrochemiluminescence (ECL). *Chem. Rev.* **2004**, *104*, 3003−3036.

(8) Guo, S.; Fabian, O.; Chang, Y.-L.; Chen, J.-T.; Lackowski, W. M.; Barbara, P. F. Electrogenerated Chemiluminescence of Conjugated Polymer Films from Patterned Electrodes. *J. Am. Chem. Soc.* **2011**, *133*, 11994−12000.

(9) Xu, L.; Li, Y.; Wu, S.; Liu, X.; Su, B. Imaging Latent Fingerprints by Electrochemiluminescence. *Angew. Chem., Int. Ed.* **2012**, *51*, 8068−8072.

(10) Chang, Y.-L.; Palacios, R. E.; Chen, J.-T.; Stevenson, K. J.; Guo, S.; Lackowski, W. M.; Barbara, P. F. Electrogenerated Chemiluminescence of Soliton Waves in Conjugated Polymers. *J. Am. Chem. Soc.* **2009**, *131*, 14166−14167.

(11) Chen, J.-T.; Chang, Y.-L.; Guo, S.; Fabian, O.; Lackowski, W. M.; Barbara, P. F. Electrogenerated Chemiluminescence of Pure Polymer Films and Polymer Blends. *Macromol. Rapid Commun.* **2011**, *32*, 598−603.

(12) Aoki, K.; Aramoto, T.; Hoshino, Y. Photographic Measurements of Propagation Speeds of the Conducting Zone in Polyaniline Films during Electrochemical Switching. *J. Electroanal. Chem.* **1992**, *340*, 127−135.

(13) Tezuka, Y.; Aoki, K.; Ishii, A. Alternation of Conducting Zone from Propagation-Control to Diffusion-Control at Polythiophene Films by Solvent Substitution. *Electrochim. Acta* **1999**, *44* 1871−1877. Workshop on the Electrochemistry of Electroactive Polymer Films (WEEPF97), Dourdan, France, Sept 22−24, 1997.

(14) Tezuka, Y.; Ohyama, S.; Ishii, T.; Aoki, K. Observation of Propagation Speed of Conductive Front in Electrochemical Doping Process of Polypyrrole Films. *Bull. Chem. Soc. Jpn.* **1991**, *64*, 2045−2051.

(15) Wang, X.; Shapiro, B.; Smela, E. Visualizing Ion Currents in Conjugated Polymers. *Adv. Mater.* **2004**, *16*, 1605−1609.

(16) Edwards, D. A. Constant Front Speed in Weakly Diffusive Non-Fickian Systems. *SIAM J. Appl. Math.* **1995**, *55*, 1039−1058.

(17) Durning, C. J.; Edwards, D. A.; Cohen, D. S. Perturbation Analysis of Thomas and Windle's Model of Case II Transport. *AIChE J.* **1996**, *42*, 2025−2035.

(18) Thomas, N.; Windle, A. A Theory of Case II Diffusion. *Polymer* **1982**, *23*, 529−542.

(19) Wang, X.; Smela, E. Experimental Studies of Ion Transport in PPy(DBS). *J. Phys. Chem. C* **2009**, *113*, 369−381.

(20) Lacroix, J.; Fraoua, K.; Lacaze, P. Moving Front Phenomena in the Switching of Conductive Polymers. *J. Electroanal. Chem.* **1998**, *444*, 83−93.

(21) Wang, X.; Shapiro, B.; Smela, E. Development of a Model for Charge Transport in Conjugated Polymers. *J. Phys. Chem. C* **2009**, *113*, 382−401.

(22) Edwards, D. A. Sharp Fickian Fronts in Conjugated Polymer Films. *IMA J. Appl. Math.*, submitted.

(23) Corless, R.; Gonnet, G.; Hare, D.; Jeffrey, D.; Knuth, D. On the Lambert W Function. *Adv. Comput. Math.* **1996**, *5*, 329−359.

(24) Sauer, T. *Numerical Analysis*, 2nd ed.; Pearson: New York, 2012.